J Mater Sci (2011) 46:670–674
DOI 10.1007/s10853-010-4789-5

Controllable growth of silver-seeded PbS nanostructures

**Yan Li · Feifei Du · Hua Zhang · Xiling Du ·
Jian Zhu · Xinhua Zhong**

Received: 4 May 2010 / Accepted: 22 July 2010 / Published online: 4 August 2010

Abstract A surfactant-assisted colloidal chemistry technique for the controllable growth of various PbS architectural nanostructures catalyzed by Ag nanocrystal seeds was reported. The sizes and morphologies of the obtained PbS nanostructures were dependent on the amount of Ag nanocrystal seeds and the ratio of Pb to S precursors. By varying the amount of Ag seed, sphere-, cube- and rod-shaped PbS nanostructures were obtained; while the morphologies changed from nano-scaled sphere to small cube and then to large truncated-cube when decreasing the precursors' ratio of Pb to S from 5:1 to 2:1 and then to 1:2 with the fixation of the amount of Ag seed. Control of morphology under different conditions has been systematically studied and the mechanism of morphology formation was also primarily discussed.

Introduction

Nanocrystals (NCs) have attracted great interest due to their fundamental size- and shape-dependent properties and many important potential technological applications [1]. The design and preparation of nanomaterials with tunable physical and chemical properties is a tremendous challenge for materials chemists. In the past decade, much effort has been devoted in the design and synthesis of uniformly sized NCs with well-defined anisotropic morphologies, because the morphology (including dimensionality and shape) of NCs determine their intrinsic physical and chemical properties [2–4]. Among these materials, lead sulfide (PbS) NCs with a small band gap (0.41 eV in bulk form at 300 K) and a large exciton Bohr radius (18 nm) have been the most extensively studied owning to their versatile envisaged applications such as sensors [5], biomedical labels [6], solar cell sensitizers, etc. [7, 8]. Recently, PbS NCs have been prepared through chemical vapor deposition method [9, 10], hydrothermal process [11], and colloidal chemical route [12–15]. Furthermore, PbS morphology control has been achieved in water by using biological bovine serum albumin and different polymer capping agents [16–18]. Although these routes were successful in synthesizing PbS nanostructures with different morphologies, it is still a challenge to tune the sizes and morphologies through a simple and effective method. The thermal decomposition of metal precursors in high-boiling-point solvents, such as amines or alcohols which act as reactants as well as control agents for crystals growth and architectural control, has been proven to be an effective route for tuning the morphology of the obtained NCs because the selected surfactants can effectively kinetically control the growth rates of various facets of nucleus, and both the reaction temperature and the chemical nature of the reaction media can tune the decomposition rate of the precursor [19–22]. Another common solution based approach to the anisotropic growth of nanostructures is the use of some noble metal particles with high-boiling point (such as Au, Ag, or Pd) as catalyst to trigger the heterogeneous nucleation and growth of anisotropic nanostructures [23–27].

Y. Li · F. Du · H. Zhang (✉) · X. Zhong (✉)
Key Laboratory for Advanced Materials Research, Department of Chemistry, East China University of Science and Technology, 200237 Shanghai, China
e-mail: zhanghjy@ecust.edu.cn

X. Zhong
e-mail: zhongxh@ecust.edu.cn

X. Du · J. Zhu
School of Life Science and Technology, Tongji University, 200092 Shanghai, China

Herein, we report an effective and convenient method for tuning PbS nanostructures with various sizes and morphologies by changing the amount of Ag NCs seed as catalyst and ratios of Pb to S precursors. The nanostructures evolved from spheres to cubes and then to rods as increasing the amount of Ag NCs seeds. The atom molar ratios of Pb to S also affected the morphologies of PbS nanostructures. The formation mechanism was also discussed.

Experimental

Chemicals

Lead oxide (99.99%), oleylamine (80–90%, OAm), 1-octadecene (90%, ODE), oleic acid (90%, OA), silver nitrate (99%), and sulfur (99.5%) were purchased from Aldrich. All chemicals were used as received without further purification. The experiments were performed using standard air-free techniques [28].

Precursor's preparation

The S precursor (0.1 M) was obtained by dissolving 32.0 mg of elemental S in 10.0 mL of ODE. Dissolution of the elemental sulfur could be completed either by ultrasonication or gentle heating at ~100 °C in a flask with stirring. The Pb precursor (0.1 M) was obtained by dissolving 244.5 mg (1 mmol) of PbO in OA (5.0 ml) and ODE (5.0 ml) at ~110 °C to get a clear solution.

Synthesis of Ag NCs seeds

27.4 mg (0.16 mmol) of $AgNO_3$ and 5 mL of OAm were loaded in a three-neck flask, and the mixture was degassed at 60 °C under a vacuum of ~1 mbar for 2–3 min under magnetic stirring. Then, the reaction vessel was filled with argon and heated to 175 °C and maintained at this temperature for 5 min. In this stage, the original colorless solution turned to brown, indicating the formation of silver NCs. Transmission electron microscope (TEM) analysis shows that the obtained spherical Ag NCs have an average size of ~7 nm.

Synthesis of PbS NCs

Typically, 1.0 mL (0.1 mmol) of Pb precursor, 4.0 mL of OAm, and 130 μL of Ag NCs solution (molar ratio of Ag/Pb = 4%) were added into a three-neck flask, and the mixture was degassed at 60 °C under a vacuum of ~1 mbar for 5 min. The reaction vessel was then filled with argon, and its temperature was raised to 140 °C and maintained at this temperature for 5 min. Then appropriate volume of S precursor solution according to the calculated molar ratio of Pb to S (1.0 mL for 1:1) was quickly injected into the flask while the temperature was allowed to decrease to some extent, and maintained at this temperature for 30 min. With the addition of S precursor, the original colorless solution turned to black immediately. Subsequently, the reaction mixture was cooled down to ~60 °C, and 10 mL of toluene were added. The nanostructures (black precipitate) were isolated and purified by centrifugation and washed with chloroform and acetone for several times. The resulted organic ligand-coated PbS NCs are re-dispersed in nonpolar solvents, such as chloroform, toluene, or hexane and used for the following measurements without any size selection.

Characterization

The sizes and morphologies of the PbS products were observed by transmission electron microscope (TEM) taken on a JEOL JEM-1400 microscope at an acceleration voltage of 100 kV. The samples were prepared by depositing a drop of dilute toluene dispersion of NCs on a carbon film coated copper grid. The purity and structure of the products were confirmed by X-ray diffraction (XRD) analysis obtained on a Philips (PW 1820) X-ray diffractometer equipped with graphite monochromatized high-intensity Cu-Kα radiation ($\lambda = 1.5406$ Å). XRD samples were prepared by depositing NCs on a piece of Si (100) wafer.

Results and discussion

Tuning the morphologies of PbS nanostructures by changing the amount of Ag NCs seed

Figure 1 shows the typical TEM images of different PbS nanostructures obtained under different amount of Ag NCs seeds when the molar ratio of Pb to S precursors was fixed at 1:1. Without the presence of Ag seed, PbS aggregated spheres (Fig. 1a) randomly composed of many small nanoparticles formed with individual particle size cannot be accurately evaluated due to aggregation but undoubtedly less than 10 nm from the present TEM image. When a small amount of Ag NCs seed was used (with Ag/Pb molar ratio of 0.4%), PbS monodispersed spheres with sizes ranging from 12 to 30 nm were obtained. When the amount of Ag seed was increased to Ag/Pb = 1%, the obtained PbS nanostructures were dominated by regular cubes with uniform shape and size in the range of 26–30 nm (shown in Fig. 1c). When the amount of Ag seed was further increased to Ag/Pb = 4%, isolated PbS nanorods having

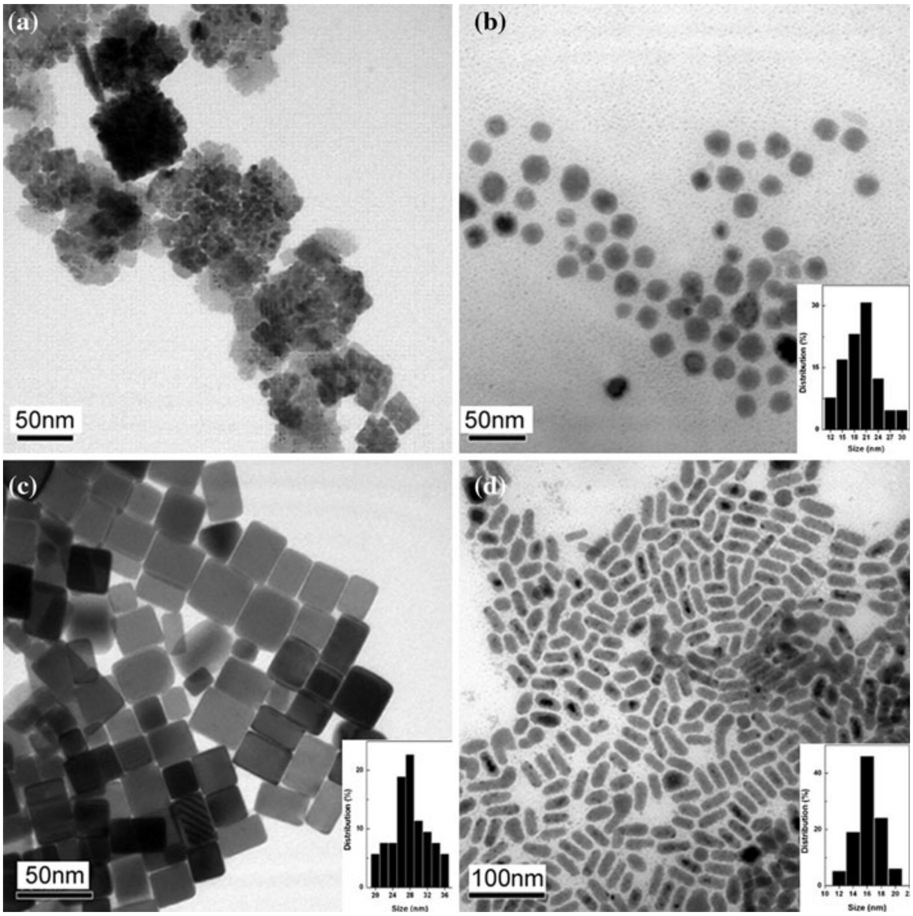

Fig. 1 TEM images of PbS nanostructures synthesized under different amount of Ag NCs seeds **a** aggregated spheres composed of small nanoparticles in the absence of Ag seeds, **b** spheres with Ag/Pb = 0.4%, **c** cubes with Ag/Pb = 1%, and **d** rods with Ag/Pb = 4%. The *insets* show the corresponding size distribution histogram

average diameter and length of ~16 ± 2 nm (size distribution shown in inset) and ~35 ± 5 nm, respectively, formed (Fig. 1d).

It is clear that when the molar ratio of Pb/S precursors was kept for 1, the amount of Ag NCs seeds is the critical parameter in determining the shape and size of PbS nanostructures. PbS nanostructures could conveniently change from aggregated nanoparticles to spheres, to cubes, and then to nanorods along with size from small to large or slightly anisotropic morphology with increasing the amount of Ag seeds.

Influences of the Pb:S ratio

To investigate the influence of the molar ratio of Pb to S precursors on the morphology of PbS nanostructures, a series of experiments were carried out under the fixed amount of Ag NCs (Ag/Pb = 4%) and other experimental parameters. Figure 2 shows the TEM images of different PbS nanostructures obtained at Pb to S precursors ratios varying from 5:1 to 2:1 and then to 1:2. When the ratio was 5:1, spheres and cubes with average diameters in the range of 8–12 nm coexisted in the products (Fig. 2a). When the Pb:S ratio was decreased to 2:1, PbS cubes with ~18 nm size formed (Fig. 2b). When the Pb:S ratio was reduced to 1:2, large PbS truncated cubes were obtained with size of ~21 ± 2 nm (Fig. 2d). Upon reviewing the size and shape dependent of experimental conditions, one can conclude that the synthesized PbS nanostructures change from sphere-, to cube-, to rod-, and then to truncated-cube-like shape with decreasing the molar ratio of Pb to S.

To further confirm the crystal structure of the samples, XRD measurement was carried out. Figure 3 shows the typical XRD pattern of PbS nanostructures prepared at Ag/Pb = 4% and Pb:S = 1:1. It should be noted that all the samples with different morphologies show a similar XRD pattern. One can see from the XRD pattern that the products are well crystallized and all the broadened peaks could be indexed as 111, 200, 220, 311, 222, 400, and 331 according to JCPDS card No 78-1901, indicating the cubic structured PbS nanostructures with the lattice constant of $a = 0.392$ nm. The amount of Ag NCs is not enough to be detected and no peaks are shown in the XRD pattern.

Growth mechanisms

The TEM results show that PbS nanostructures with a variety of morphologies could be well controlled by tuning

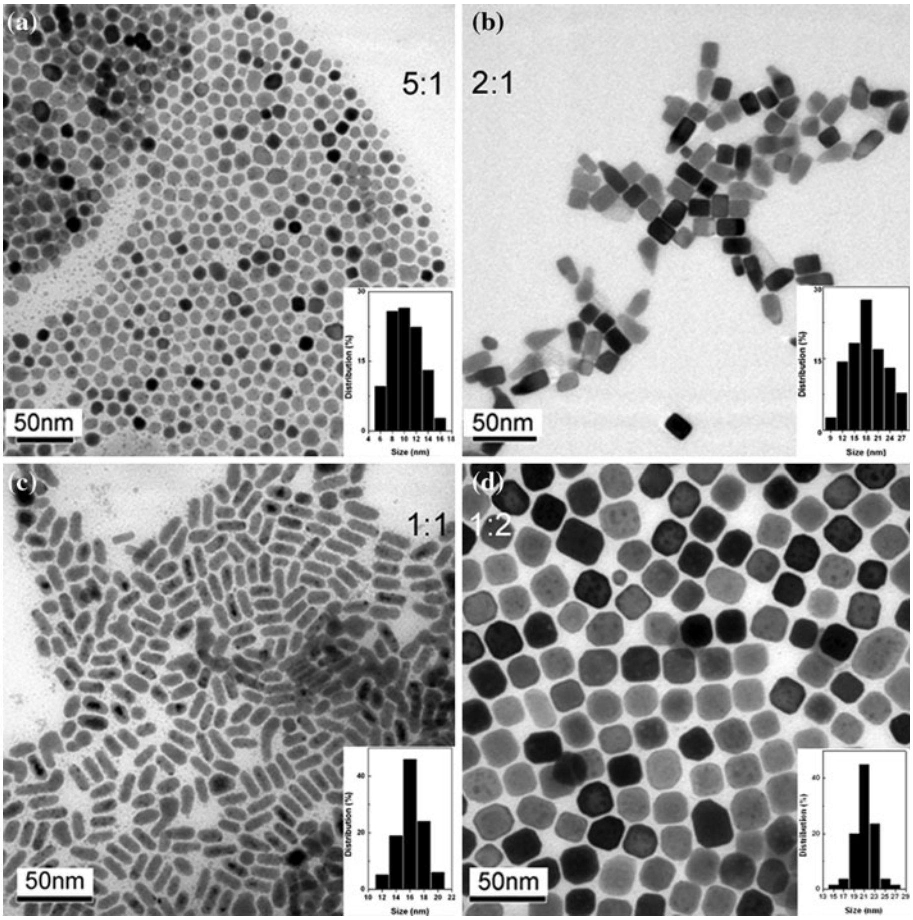

Fig. 2 TEM images of different PbS nanostructures synthesized at different molar ratios of Pb to S precursors (shown as *legends* in the corresponding images) with fixation of the amount of Ag NCs at Ag/Pb = 4%. The *insets* show the corresponding size distribution histogram

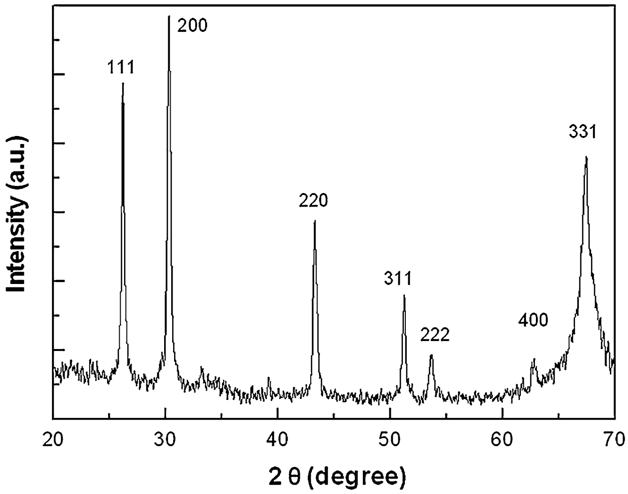

Fig. 3 XRD pattern of PbS nanostructures prepared at Ag/Pb = 4% and Pb:S = 1:1

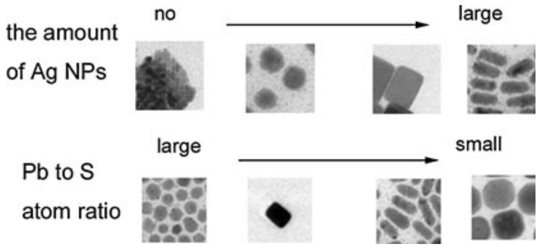

Fig. 4 The relationship of PbS NC morphologies with the amount of Ag seeds and the Pb to S ratio

the experimental conditions including Ag seed amount and precursors' ratio of Pb to S with the summary shown in Fig. 4. The formation of various shaped PbS nanostructures should result from changes in the PbS NCs nucleation and growth kinetics in the presence of Ag NCs seed. It is well known that the crystalline phase of the nucleus at the nucleating stage is critical in directing the NC shapes. Once NC seeds formed with a specific crystalline phase, several other factors, including intrinsic surface energy of different crystallographic surfaces, the balance between thermodynamic and kinetic growth regime will affect the final geometry of NCs during the crystal growth process [24]. The crystal surface energy was identified as the main driving force for the growth of anisotropic nanostructures and can be modulated by the use of surface-selective capping molecules [25]. In the previous work [16–18], the authors thought that the capping agents could selectively adsorbed on the {111} facets of noble metals such as Ag and the cubic structured PbS other than the {100} and {110} planes. In consequence, the {111} facets will be passivated and {100} planes grow preferentially which could also be favored by the higher concentration of surfactant. We think that it is similar to our experimental results. In our experiments, OAm plays an important role in formation of PbS nanostructures, and serves as solvent as well as a capping molecule for architectural control. Aggregated PbS NCs were observed in the absence of Ag NCs seeds due to the nucleation, growth and congregation occurred in solution. When the not purified OAm-capped Ag NCs in OAm were introduced to the reaction system, they served as a template and nucleation sites, resulting the monodispersed PbS NCs [23, 24]. When the NCs grew to a certain size, the PbS NCs detached from Ag and OAm was absorbed on the {111} facets. The introduced different amount of OAm-capped Ag seed from small to large resulting in the concentration of surfactant from small to large finally led to the PbS morphology from sphere- to cube- then to rod-shaped nanostructures. As to the effect of molar ratio of Pb to S, Prasad and his coworkers [12, 14] have reported the growth mechanism associated with depletion of precursors in which depletion of precursors on each seed particle would make the different growth rate on some facets, sometimes allow anisotropic growth along a specific direction to form rods or wires. Under our constant concentration of Pb precursor, the molar ratio of Pb to S from high to low represents the concentration of S precursors changing from low to high. When the S precursor was seriously insufficient, the small PbS NCs had no enough time for continuous growth along a specific direction. Then the PbS smaller spheres were obtained. As increasing the precursor's concentration and under the passivation of {111} facets by OAm, the continuous growth along {100} facets was possible, and cubes, rods, or truncated cubes formed. How the morphology evolves upon seriously rich S precursors injected should be further studied next.

Conclusions

A facile hot colloidal metallic seed catalyzed method was developed, which effectively provides control of the shape, size, and structure of PbS NCs by manipulating the synthesis parameters, such as the amount of the seeds and the precursor ratios. PbS nano-scaled spheres, cubes, and rods were obtained when the amount of seeds changed from small to large and the atom molar ratio of Pb to S changed from large to small. The growth mechanisms associated with selective absorption of surfactant and depletion of precursors could explain the morphology evolution. The seeds catalyzed growth may be applied to control a variety of compounds through solution method.

Acknowledgements We thank the National Natural Science Foundation of China (nos. 20871047, 20771037), the Program for New Century Excellent Talents in University of China (NCET-06-0417), Pujiang Talents Project (07pj14032), Shuguang Project (06SG33), and SRFDP (20070251014) for financial supports.

References

1. Burda C, Chen XB, Narayanan R, EI-Sayed MA (2005) Chem Rev 105:1025
2. Puntes VF, Krishnan KM, Alivisatos AP (2001) Science 291:2115
3. Yin S, Akita SG, Shinozaki M, Li RX, Sato T (2008) J Mater Sci 43:2234. doi:10.1007/s10853-007-2070-3
4. Xia YN, Yang PD, Sun YG, Wu Y, Mayers B, Gates B, Yin Y, Kim F, Yan H (2003) Adv Mater 15:353
5. Zhang ZH, Lee SH, Vittal J, Chin WS (2006) J Phys Chem B 110:6649
6. Brumer M, Kigel A, Amirav L, Sashchiuk A, Solomesch O, Tessler N, Lifshitz E (2005) Adv Funct Mater 15:1111
7. Ellingson RJ, Beard MC, Johnson JC, Yu PR, Micic O, Nozik AJ, Shabaev A, Efros AL (2005) Nano Lett 5:865
8. Mokari TL, Zhang MJ, Yang PD (2007) J Am Chem Soc 129:9864
9. Afzaal M, O'Brien P (2006) J Mater Chem 16:1113
10. Zhang H, Zuo M, Tan S, Li GP, Zhang SY (2006) Nanotechnology 17:2931
11. Roman-Zamorano JF, Flores-Acosta M, Arizpe-Chavez H, Castillon-Barraza FF, Farias MH, Ramirea-Bon R (2009) J Mater Sci 44:4781. doi:10.1007/s10853-009-3720-4
12. Yong KT, Sahoo Y, Choudhury KR, Swihart MT, Minter JR, Prasad PN (2006) Chem Mater 18:5965
13. Lee SM, Jun Y, Cho SN, Cheon J (2002) J Am Chem Soc 124:11244
14. Yong KT, Sahoo Y, Choudhury KR, Swihart MT, Mint JR, Prasad PN (2006) Nano Lett 6:709
15. Talapin DV, Yu H, Shevchenko EV, Lobo A, Murrray CB (2007) J Phys Chem C 111:14049
16. Bakshi MS, Thakur P, Kaur G, Kaur H, Banipal TS, Possmayer F, Petersen NO (2009) Adv Func Mater 111:1451
17. Bakshi MS, Kaur G, Possmayer F, Petersen NO (2008) J Phys Chem C 112:4948
18. Bakshi MS, Thakur P, Sachar S, Kaur G, Banipal TS, Possmayer F, Petersen NO (2007) J Phys Chem C 111:18087
19. Jun YW, Lee SM, Kang NJ, Cheon J (2001) J Am Chem Soc 123:5150
20. Zhong X, Feng Y, Lieberwirth I, Knoll W (2006) Chem Mater 18:2468
21. Zhong X, Feng Y, Zhang Y, Lieberwirth I, Knoll W (2007) Small 3:1194
22. Jun YW, Jung YY, Cheon J (2002) J Am Chem Soc 124:615
23. Teng XW, Yang H (2005) Nano Lett 5:885
24. Shi WL, Zeng H, Sahoo Y, Ohulchanskyy TY, Ding Y, Wang ZL, Swihart MT, Prasad PN (2006) Nano Lett 6:875
25. Chen CY, Lee JR, Chia CT, Lu CR, Liu IS, Su WF (2008) J Phys Chem Solids 69:629
26. Fang Z, Zhang YL, Du FF, Zhong XH (2008) Nano Res 1:249
27. Basavalingu B, Byrappa K, Yoshimura M, Madhusudan P, Dayananda AS (2006) J Mater Sci 41:1465
28. Du FF, Zhang H, Du XL, Zhu J, Zhong XH (2010) Mater Chem Phys 121:118